https://doi.org/10.17221/285/2024-PSE

# Innovative approach to utilising magnetic fields to enhance wheat yield: evidence from field studies in China

*Yinglei Zhang[1,3], Hangyu Dou[1], Liuyang Yang[1], Yihan Zhang[1], Wei Sun[1], Yihao Ruan[1], Jiameng Guo[1,3], Yongchao Wang[1,3], Ruixin Shao[1,3], Qinghua Yang[1,2,3]*, Hao Wang[1,3]**

[1]*College of Agronomy, Henan Agriculture University, Zhengzhou, Henan, P.R. China*
[2]*Engineering Research Center for Crop Chemical Regulation, Zhengzhou, Henan, P.R. China*
[3]*Key Laboratory of Regulating and Controlling Crop Growth and Development Ministry of Education, Zhengzhou, Henan, P.R. China*

**Corresponding authors: yangqinghua@henau.edu.cn; wanghaonxy@163.com*

**Citation:** Zhang Y.L., Dou H.Y., Yang L.Y., Zhang Y.H., Sun W., Ruan Y.H., Guo J.M., Wang Y.C., Shao R.X., Yang Q.H., Wang H. (2024): Innovative approach to utilising magnetic fields to enhance wheat yield: evidence from field studies in China. Plant Soil Environ., 70: 656–672.

**Abstract:** Magnetic fields, as a form of physical energy, exert an influence on biological activities. However, our current understanding of the impact of magnetic fields on wheat yield remains limited. In this study, our objective was to investigate the effects of magnetic field treatment of wheat plants on their yield, root growth, absorption of nitrogen and phosphorus and soil bacterial diversity. The experiments were conducted at two agricultural research stations in China, Zhengzhou and Xuchang. Plants were treated with magnetic fields of 20, 40, 60, and 80 mT induced by permanent magnets for chronic exposure. Untreated plants were considered as controls. Our result showed that soil nutrients were found to have a substantial impact on wheat nitrogen and phosphorus absorption, and wheat nitrogen and phosphorus absorption significantly affected wheat yield. The change in soil nutrient content was caused by the change in soil bacterial community diversity and abundance, and increased soil nutrients increased wheat yield. The results suggest that magnetic field treatment stimulated wheat plant growth and yield, and changed soil nutrient content through improved soil bacterial community diversity and increased soil nitrogen and phosphorous absorption.

**Keywords:** soil rhizosphere nutrients; microbial community; nitrogen nutrient absorption; phosphorus nutrient absorption

Wheat, one of the most important crops worldwide, faces the challenge of increasing yields while minimising environmental pollution. The excessive use of mineral fertilisers in current farming practices not only results in inefficient fertiliser utilisation but also contributes to various environmental issues (Dai et al. 2022, Zhang et al. 2022). To address this problem, it is crucial to explore alternative approaches that can enhance field production while reducing reliance on chemical elements and mitigating environmental pollution.

Magnetic fields, a form of physical energy that surrounds us in our daily lives, have been found to exert an influence on living organisms on Earth. Previous studies have demonstrated the potential of magnetic fields to promote crop growth, resulting in increased plant development and improved yield (Alpsoy and Unal 2019). Studies focusing specifically on wheat have shown that magnetic field treatments can enhance seed germination and stimulate wheat growth (Pietruszewski and Kania 2010). Moreover, investigations into the physiological changes induced

https://doi.org/10.17221/285/2024-PSE

by magnetic fields have indicated that improved antioxidant systems and enhanced photosynthesis play a role in promoting wheat growth and increasing yield (Ghanati and Payez 2015, Sukhov et al. 2021). Additionally, magnetic field treatments have been shown to act as a form of energy that mitigates the harmful effects of stress. For example, extremely low-frequency magnetic fields have been proven to modify wheat's resistance to adverse drought conditions (Mshenskaya et al. 2023). Furthermore, when exposed to heavy metals, such as cadmium and lead, magnetic field treatments have been found to ameliorate the physiological effects on young wheat seedlings (Chen et al. 2017). These studies highlight the important role of magnetic fields as a form of physical energy in promoting wheat growth and development. By harnessing the potential of magnetic fields in agricultural practices, it is possible to increase wheat yields while reducing reliance on mineral fertilisers and minimising environmental pollution. Implementing magnetic field treatments represents a promising avenue for achieving sustainable and environmentally friendly agricultural production.

The enhancement of soil nutrient status emerges as a crucial factor influencing wheat growth. Nitrogen and phosphorus are essential nutrients for wheat, and their availability significantly impacts nutrient absorption and plant development. Prior studies have demonstrated that increasing nitrogen availability contributes to higher wheat yields (Liu et al. 2013). Similarly, the application of phosphorus fertilisers and the improved utilisation efficiency of phosphate fertilisers have been shown to stimulate wheat growth (Covacevich et al. 2007). Plants primarily obtain nitrogen and phosphorus from the soil, and microorganisms play a fundamental role in soil nutrient cycling. They actively participate in soil nitrogen conversion processes (Kuypers et al. 2018) and the phosphorus cycle (Zhouchang et al. 2023). Soil bacteria, specifically, significantly influence nutrient conversion (Merloti et al. 2019). Therefore, it is imperative to consider bacterial factors when studying the effects of magnetic fields on nutrient availability. Research has indicated that microorganisms can engage in processes such as nitrification, nitrogen fixation, and denitrification, thereby enhancing the nutrient utilisation efficiency of the soil and promoting crop growth (Zhang et al. 2019). However, the specific impact of magnetic fields on nutrient availability and bacterial communities in wheat fields and their subsequent influence on wheat yield remain understudied.

In addition, plant roots serve as vital sites for nutrient uptake from the soil and establish a dynamic interaction with microbial activities, forming the rhizosphere, significantly affecting soil nutrient conversion processes (Song et al. 2020, Trivedi et al. 2021). Consequently, the nutrient cycling process within the rhizosphere soil exhibits heightened activity, thereby necessitating thorough attention to rhizosphere processes when investigating soil nutrient transformations.

The present study aimed to evaluate the impact of magnetic field treatment on various factors, including wheat yield, root growth, soil properties, and soil microbial activity, as well as the interconnections between them. The following four hypotheses were formulated to guide the present study. (1) Magnetic field treatment enhances wheat growth, yield, and yield composition; (2) magnetic field treatment increases or sustains the availability of essential soil nutrients, such as $NH_4^+$-N, $NO_3^-$-N, and available phosphorus; (3) changes in soil bacteria diversity are the primary driver behind the increase in soil nutrient content, ultimately leading to enhanced wheat yield, and (4) magnetic field treatment stimulates wheat root growth, facilitating increased wheat nitrogen and phosphorus absorption.

These hypotheses served as the foundation for our investigation into the effects of magnetic field treatment on wheat and its associated soil and microbial attributes. By analysing the data and assessing the observed outcomes, we aimed to gain insights into the potential benefits and mechanisms underlying the use of magnetic fields in agricultural practices.

## MATERIAL AND METHODS

**Site description Site 1**. The field experiment was conducted on farmland at the Zhengzhou Agricultural Research Station in Zhengzhou City, Henan Province, China. The specific coordinates of the site are 34°6'15.88"N, 113°52'41.76"E, and the elevation is approximately 80 m a.s.l. The region experiences a temperate monsoon climate characterised by an average annual precipitation of 633 mm and an average annual temperature of 13.2 °C. According to the International Classification of Soil Science, the soil type at this location is classified as Anthrosols. The measured soil characteristics in this area are as follows: soil organic matter content, 7.2 g/kg; total nitrogen content, 0.5 g/kg; available phosphorus content, 5.6 mg/kg and available potassium content, 22.0 mg/kg.

https://doi.org/10.17221/285/2024-PSE

**Site 2.** The field experiment was conducted on farmland at the Xuchang Agricultural Research Station in Xuchang City, Henan Province, China. The precise coordinates of the site are 34°8'15.23"N, 113°36'38.76"E, and the elevation is approximately 80 m a.s.l. The region is characterised by a temperate monsoon climate, with an average annual precipitation of 579 mm and an average annual temperature of 16.8 °C. According to the International Classification of Soil Science, the soil at this location is classified as Anthrosols. The measured soil characteristics in this area are as follows: soil organic matter content, 10.28 g/kg; total nitrogen content, 0.972 g/kg; and available phosphorus content, 89.7 mg/kg.

**Experimental design.** A two-site experiment was conducted following a randomised complete block design with five treatments and three replicates. The five magnetic field intensity treatments were 0, 20, 40, 60, and 80 mT, with 0 mT serving as the control (CK). Each experimental plot had dimensions of 5 × 5 m, and boundary plots were created by leaving a 1 m margin around the experimental field to eliminate border effects. Weeds within the plots were controlled using pre-emergence herbicides.

The study utilised the wheat cv. Zhoumai 40, which is commonly grown by local farmers. The crop planting density adhered to local production practices, with wheat planted with a 15 cm inter-row spacing and a plant spacing of 10 cm. The sowing depth ranged from 3 to 5 cm. Fertiliser application to wheat was based on local farmers' standards. Specifically, the nitrogen application rate for wheat was 200 kg/ha, while the amount of phosphorus and potassium applied to all plots was 120 kg/ha and 90 kg/ha, respectively. Adequate irrigation was provided to the wheat throughout the growing season.

The magnet utilised in the experiment was a black bar magnet of different sizes securely wrapped in polyethylene plastic before being buried in the ground. This protective measure was implemented to prevent contact of metal elements within the magnet with the soil. Before commencing the treatment, the magnetic field strength was accurately measured using a high-precision Hall probe purchased from Beijing Cuihai Jiacheng Magnetoelectric Technology Co., Ltd. To ensure uniform magnetic field treatment across all wheat plants, the bar magnets were positioned between two rows of wheat, with one row magnet placed in two rows (Figure 1). This arrangement guaranteed that all wheat plants received equal and consistent magnetic field exposure. The magnets used for both sites remained the same in both years of cultivation. The field management practices and cultivation techniques were consistent across both sites.

**Sample collection.** The field experiment divided soil samples into rhizosphere and bulk soil and collected them at the wheat heading and ripening stages. Rhizosphere soil samples were collected using the root-shaking method (Barillot et al. 2013), and the soil attached to the rhizosphere was gently brushed off with a sterile brush. The sterilised mesh screen with a 2 mm aperture was then completely and evenly dispersed in the centrifuge tube. The bulk soil was collected far from the rhizosphere between the two rows of wheat at depths of 0–10, 10–20, and 20–30 cm. Part of the sample was placed in a centrifuge tube, and part was stored in a 4 °C cooler and brought back to the laboratory for further measurements. Plant samples were collected at the heading and ripening stages to measure biomass, and the plants were dried and crushed at the ripening stage to determine the plants' total nitrogen and phosphorus content. Wheat roots were collected gently at the heading stage, minimising root damage, and rinsed in sterile water. One part was utilised for root scanning, while the other part was placed in an FAA fixative solution to make root slices to observe the fine structure of the root system. Slices are taken from 5–8 cm of the secondary root of wheat near the root tip.

## Measurements

**Yield and dry matter**. Grain yield was measured at the physiological ripening stage of wheat from both sites. The spike number was determined by conducting a sampling survey with an area of 3 $m^2$ in each

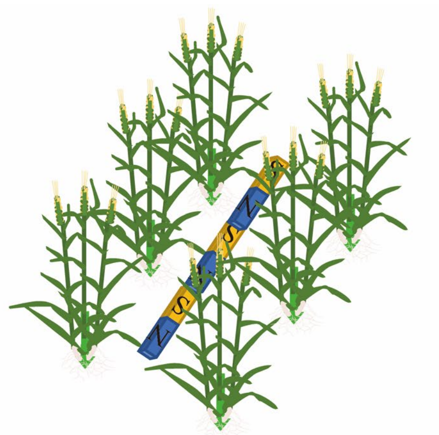

Figure 1. Distribution of magnetic field in field experiment

https://doi.org/10.17221/285/2024-PSE

plot. Additionally, 30 similar plants were randomly selected to determine dry matter, grain number per spike, and 1 000-grain weight. The samples were baked in an oven at 105 °C for 30 min and then at 80 °C for 48 h until a constant weight was achieved. The grain yield, straw yield, and 1 000-grain weight were adjusted to a moisture content of 14% (Yan et al. 2020, Arata et al. 2023, Jyolsna et al. 2024).

**Soil analysis.** The sampled soil was air-dried in a cool place and passed through 0.2-mm mesh screens to determine subsequent indexes. The soil $NO_3^-$-N and $NH_4^+$-N content was determined following Fu et al. (2019), using a continuous flow analyser (AA3, Analytical, Bran-Luebbe, Norderstedt, Germany) with 1 mol/L KCL extract. The soil available phosphorus (AP) content was determined using 0.5 mol/L $NaHCO_3$ extraction, followed by the molybdenum-antimony resistance colourimetric method (Olsen 1954).

**Wheat root analysis.** Wheat roots were scanned immediately after being brought back to the laboratory. A plant root scanner, LD-WinRHIZO, was used to perform root scans, which were then analysed using standard WinRHIZO analysis software (WinRhizo ProVision 5.0, Québec, Canada).

Wheat root slices were prepared using Yihan's method (Zhang et al. 2024). The FAA-fixed wheat roots were cut into 1 × 0.5 cm segments and rinsed with deionised water for 24 h. They were then softened with 12% hydrofluoric acid for 3 days and rinsed again with deionised water for about 48 h. (2) Samples were stained with 1% safranin solution for 48 h before dehydration using ethanol. (3) The samples were passed through a mixture of absolute ethanol and xylene (1:1) -xylene 1-xylene 2 for 1 h in each stage. (4) The material was transferred from the tissue embedding box to a small bottle, and a small amount of xylene was added to drown the material and paraffin. The waxing temperature gradually increased. (5) After the embedded sample was soaked in water for about 10 h, a slicer was used to cut the samples into slices, and a slide was prepared and observed under a microscope. Images were captured using a Leica biological microscope, and the magnification is shown in Figure 9 and; the scale is 100 μm, and the magnification is 40 ×.

**Wheat nitrogen and phosphorus content.** The wheat phosphorous content was determined using crushed plant samples following complete sulfuric/perchloric acid digestion (Chen et al. 2012). The wheat nitrogen content was analysed after Kjeldahl digestion and was determined using a continuous flow analyser (AA3,Analytical, Bran-Luebbe, Norderstedt, Germany) (Chen et al. 2012).

**Soil bacterial analysis.** Microbial community genomic DNA was extracted from 0.5 g fresh soil samples using an E.Z.N.A.® soil DNA Kit (Omega Bio-tek, Norcross, USA) according to the manufacturer's instructions. The bacterial 16S rRNA gene was amplified with primer pairs 338F (5'-ACTCCTACGGGAGGCAGCAG-3') and 806R (5'-GGACTACHVGGGTWTCTAAT-3') using an ABI GeneAmp® 9700 PCR thermocycler (ABI, Foster City, USA). The PCR mixture contained 4 μL 5 × TransStart FastPfu buffer, 2 μL 2.5 mmol dNTPs, 0.8 μL forward primer (5 μmol), 0.8 μL reverse primer (5 μmol), 0.4 μL TransStart FastPfu DNA Polymerase, 10 ng template DNA, and enough $ddH_2O$ to reach a volume of 20 μL. PCR reactions were performed in triplicate. The PCR product was extracted from 2% agarose gel, purified using an AxyPrep DNA Gel Extraction Kit (Axygen, Corning, USA) according to the manufacturer's instructions, and quantified using a Quantus™ Fluorometer (Promega, Madison, USA). Purified amplicons were pooled in equimolar proportions, and paired-end sequenced on an Illumina MiSeq PE300 platform/NovaSeq PE250 platform (Illumina, San Diego, USA) according to the standard protocols of Majorbio Bio-Pharm Technology Co. Ltd. (Shanghai, China).

**Statistical analysis.** Statistical analysis for all metabolites was performed using IBM SPSS 20.0 software (IBM, New York, USA), employing analysis of variance (ANOVA) and multiple mean comparisons ($LSD_{0.05}$) test. To visualise the data, histograms, boxplots, and correlation plots were generated using the Origin software package (version 2022, https://www.originlab.com/). The network map was generated at Gephi (Zurich, Switzerland). The Majorbio Biocloud platform was employed for the microbial data analysis. This platform, accessible at https://www.majorbio.com/en/cloud, facilitated the analysis of the microbial data. Structural equation modelling (SEM) analysis (De et al. 2018) was employed to identify soil nutrients' direct and indirect influences on wheat yield under magnetic field treatment. SEM was performed using Lisrel (linear structural relations) 8.80, a statistical software package (IBM, New York, USA). Before SEM analysis, the bivariate relationships between all variables with simple linear regressions were firstly checked to ensure the appropriateness of the linear models. The general fit of the model was verified by indices including low

https://doi.org/10.17221/285/2024-PSE

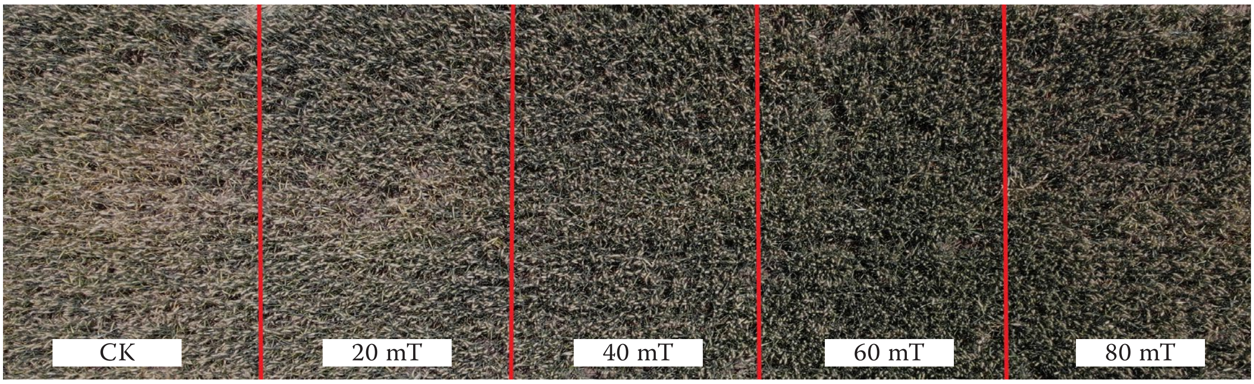


Figure 2. Aerial view of wheat growth at heading stage in Xuchang. CK – control

chi-square ($\chi^2$), probability level ($P > 0.05$), comparative fit index (CFI > 0.9), and root square mean error of approximation (RSMEA < 0.05). Different standardised path coefficients are used to indicate the relative importance of all variables to CPMI.

## RESULTS

**Wheat biomass, yield, and yield components.** At the two test sites, the application of magnetic field treatment had a significant positive impact on wheat growth (Figure 2). Comparison with CK revealed that when the magnetic field intensity reached 40 and 60 mT, the growth status of wheat showed a significant promotional effect, as evidenced by the aerial maps of wheat growth. Furthermore, the pictures of wheat growth at the ripening stage demonstrated the substantial promotion of wheat growth due to the magnetic field treatment (Figure 3).

Magnetic field treatment significantly increased the wheat growth rates at the two sites (Figure 4A, B). At the Zhengzhou and Xuchang sites, wheat growth rates were the fastest at stage 3 (heading-ripening stage). We analysed wheat biomass at stage 3, the heading and ripening stage. At the Zhengzhou site, wheat biomass increased by 19.03% and 22.52% at the heading stage and 17.76% and 22.11% at the ripening stage with 40 and 60 mT treatments, respectively, compared to CK. At the Xuchang site, wheat biomass increased by 9.63% and 13.81% at the heading stage and 11.46% and 16.45% at the ripening stage with 40 and 60 mT treatments, respectively, compared to CK.

At the Zhengzhou site, with the increase in magnetic field intensity, wheat yield showed a trend of first increasing and then decreasing, reaching a peak at 60 mT, which showed a yield increase of 15.27% compared to CK. When the magnetic field intensity reached 40 and 80 mT, the wheat yield increased by 13.8% and 8.2%, respectively. Further analysis of the yield components found that, compared with CK, under the 40 and 60 mT magnetic field treatments, the wheat ear length increased by 6.2% and 7.4%, respectively. The ear coarse increased by 10.3% under the 40 mT treatment, and the 1 000-grain weight increased by 5.3% under the 60 mT treatment (Table 1).

In Xuchang, wheat yield increased by 19.2% compared with CK, reaching a peak at 40 mT. Under mag-


Figure 3. Wheat growth at ripening stage in Xuchang. CK – control

https://doi.org/10.17221/285/2024-PSE

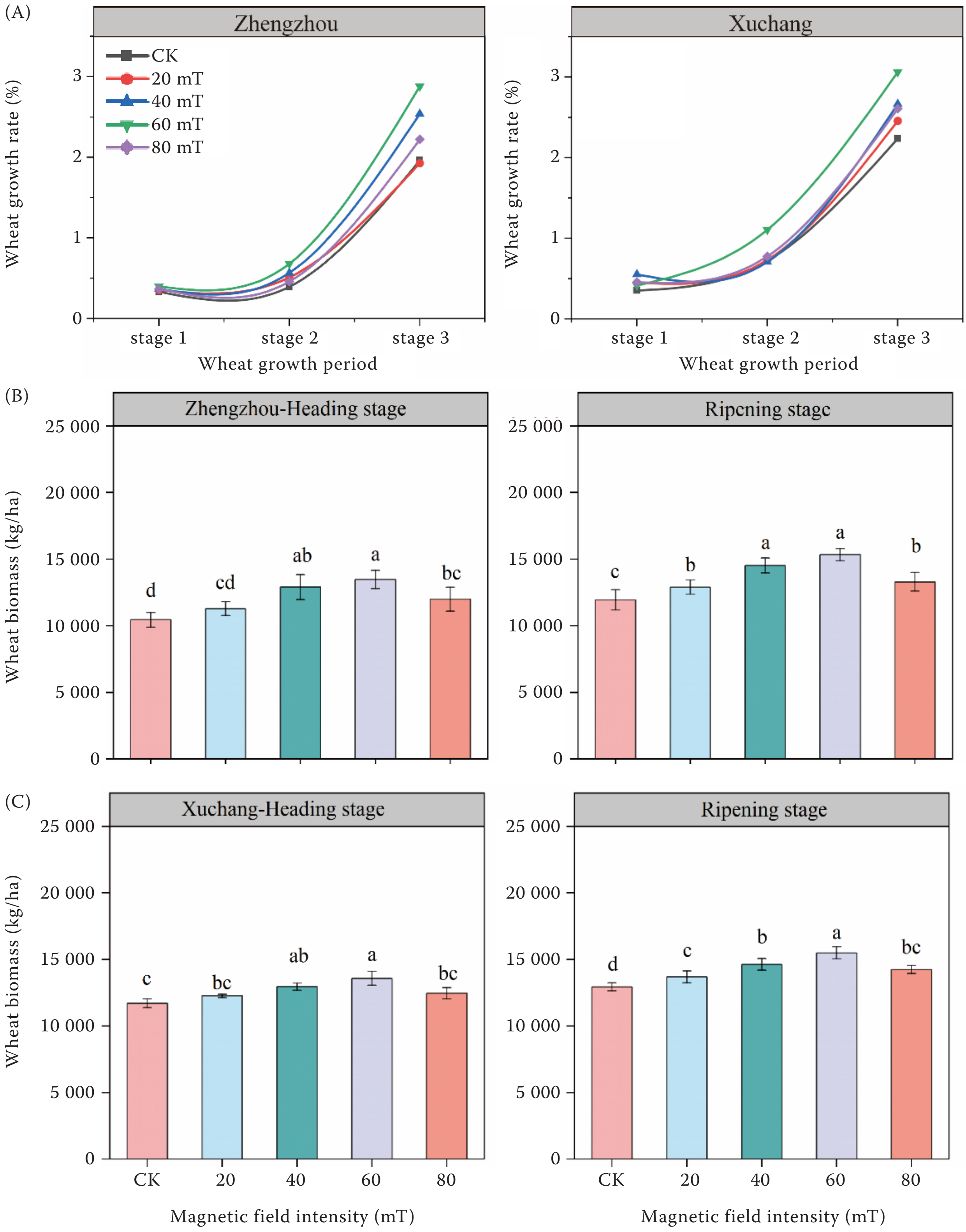


Figure 4. Wheat biomass at the heading and ripening stage. (A) The growth rate of wheat from regreening to the ripening stage in Zhengzhou and Xuchang. Stage 1 – regreening-jointing; stage 2 – jointing-heading; stage 3 – heading-ripening; (B) wheat biomass at heading and ripening stage, and (C) heat biomass at heading and ripening stage different letters above the columns mean indicating significant differences ($P < 0.05$) between treatments. CK – control

https://doi.org/10.17221/285/2024-PSE

Table 1. Wheat grain yield and yield components for different magnetic field treatments in two sites

| | Treatment | Ear length (cm) | Ear coarse (mm) | Spikes number | Kernels per spike | 1 000-grain weight (g) | Grain yield (kg/ha) |
|---|---|---|---|---|---|---|---|
| Zhengzhou | CK | 9.35 ± 0.21$^{c}$ | 8.38 ± 0.21$^{b}$ | 487$^{d}$ | 31$^{c}$ | 47.20 ± 0.14$^{b}$ | 6 357 ± 177$^{c}$ |
| | 20 mT | 9.60 ± 0.17$^{bc}$ | 8.53 ± 0.21$^{ab}$ | 503$^{cd}$ | 32$^{bc}$ | 47.25 ± 0.11$^{b}$ | 6 677 ± 182$^{b}$ |
| | 40 mT | 9.97 ± 0.18$^{ab}$ | 9.34 ± 0.42$^{a}$ | 593$^{b}$ | 37$^{a}$ | 48.30 ± 0.02$^{ab}$ | 7 371 ± 155$^{a}$ |
| | 60 mT | 10.10 ± 0.16$^{a}$ | 8.94 ± 0.19$^{ab}$ | 633$^{a}$ | 39$^{a}$ | 49.85 ± 0.07$^{a}$ | 7 502 ± 175$^{a}$ |
| | 80 mT | 9.79 ± 0.17$^{abc}$ | 8.68 ± 0.58$^{ab}$ | 527$^{c}$ | 34$^{b}$ | 47.45 ± 0.06$^{b}$ | 6 926 ± 104$^{b}$ |
| ANOVA | F | 5.608 | 2.263 | 42.659 | 12.574 | 17.168 | 103.486 |
| | P | 0.043* | ns | < 0.0001* | < 0.0001** | 0.004* | < 0.0001** |
| Xuchang | CK | 9.38 ± 0.30$^{b}$ | 8.86 ± 0.30$^{c}$ | 527$^{c}$ | 36$^{d}$ | 47.88 ± 0.08$^{b}$ | 7 135 ± 153$^{c}$ |
| | 20 mT | 9.39 ± 0.13$^{b}$ | 8.87 ± 0.28$^{c}$ | 572$^{b}$ | 43$^{b}$ | 48.03 ± 0.33$^{b}$ | 7 537 ± 196$^{bc}$ |
| | 40 mT | 9.66 ± 0.28$^{ab}$ | 9.78 ± 0.12$^{b}$ | 611$^{a}$ | 44$^{b}$ | 50.27 ± 0.02$^{a}$ | 8 833 ± 177$^{a}$ |
| | 60 mT | 10.31 ± 0.29$^{a}$ | 9.78 ± 0.23$^{a}$ | 594$^{ab}$ | 47$^{a}$ | 48.77 ± 0.50$^{b}$ | 8 669 ± 248$^{a}$ |
| | 80 mT | 9.56 ± 0.25$^{b}$ | 9.05 ± 0.27$^{c}$ | 575$^{b}$ | 39$^{c}$ | 48.43 ± 0.82$^{b}$ | 7 893 ± 274$^{b}$ |
| ANOVA | F | 4.327 | 7.275 | 16.789 | 37.375 | 8.866 | 23.018 |
| | P | ns | 0.026* | 0.004* | 0.001** | 0.017* | 0.002* |

Different lowercase letters in the same column at the same soil depth indicate significant differences. Significance levels are as follows: *$P$ < 0.05; **$P$ < 0.01

netic field intensities of 20, 60, and 80 mT, it increased by 5.3, 17.7, and 9.6%, respectively. Compared with CK, under the 40 and 60 mT magnetic fields, the wheat ear length increased by 2.9% and 8.9%, respectively, and the ear coarse increased by 9.3% and 9.36%, respectively. Compared with CK, the spike number increased by 13.8% and the 1 000-grain weight increased by 4.8% with 40 mT magnetic field treatment (Table 2).

Table 2. Soil nutrient contents in Zhengzhou of bulk soil

| Soil depth | Treatment | HS-AP | RS-AP | HS-$NH_4^+$ | RS-$NH_4^+$ | HS-$NO_3^-$ | RS-$NO_3^-$ |
|---|---|---|---|---|---|---|---|
| 0–10 cm | CK | 6.36 ± 0.31$^{a}$ | 5.86 ± 0.23$^{a}$ | 13.45 ± 1.73$^{ab}$ | 5.08 ± 0.50$^{a}$ | 5.93 ± 0.57$^{a}$ | 6.31 ± 0.46$^{a}$ |
| | 20 mT | 6.37 ± 0.52$^{a}$ | 5.85 ± 0.25$^{a}$ | 14.12 ± 0.96$^{a}$ | 5.26 ± 1.27$^{a}$ | 6.03 ± 0.48$^{a}$ | 6.38 ± 0.55$^{a}$ |
| | 40 mT | 6.58 ± 0.75$^{a}$ | 5.85 ± 0.30$^{a}$ | 15.00 ± 1.33$^{a}$ | 5.40 ± 1.11$^{a}$ | 6.17 ± 0.78$^{a}$ | 6.09 ± 0.41$^{a}$ |
| | 60 mT | 6.86 ± 0.90$^{a}$ | 6.07 ± 0.64$^{a}$ | 14.65 ± 1.85$^{a}$ | 5.99 ± 0.41$^{a}$ | 6.06 ± 0.59$^{a}$ | 6.31 ± 0.23$^{a}$ |
| | 80 mT | 6.56 ± 0.75$^{a}$ | 5.99 ± 0.32$^{a}$ | 12.19 ± 1.03$^{b}$ | 5.06 ± 0.66$^{a}$ | 6.25 ± 0.81$^{a}$ | 6.51 ± 0.67$^{a}$ |
| 10–20 cm | CK | 6.14 ± 0.64$^{a}$ | 5.94 ± 0.34$^{a}$ | 13.30 ± 1.22$^{b}$ | 5.19 ± 0.41$^{a}$ | 5.57 ± 0.08$^{a}$ | 6.20 ± 0.65$^{a}$ |
| | 20 mT | 6.22 ± 0.59$^{a}$ | 5.90 ± 0.17$^{a}$ | 13.84 ± 1.29$^{ab}$ | 5.29 ± 0.99$^{a}$ | 5.67 ± 0.16$^{a}$ | 6.58 ± 0.52$^{a}$ |
| | 40 mT | 6.61 ± 0.27$^{a}$ | 6.04 ± 0.65$^{a}$ | 15.58 ± 0.97$^{a}$ | 5.83 ± 0.69$^{a}$ | 5.86 ± 0.42$^{a}$ | 6.80 ± 0.63$^{a}$ |
| | 60 mT | 6.47 ± 0.92$^{a}$ | 5.86 ± 0.40$^{a}$ | 14.83 ± 1.49$^{b}$ | 5.25 ± 0.91$^{a}$ | 5.62 ± 0.05$^{a}$ | 6.81 ± 0.82$^{a}$ |
| | 80 mT | 6.23 ± 0.32$^{a}$ | 5.78 ± 0.10$^{a}$ | 13.60 ± 1.61$^{b}$ | 5.13 ± 0.85$^{a}$ | 5.64 ± 0.09$^{a}$ | 6.25 ± 0.76$^{a}$ |
| 20–30 cm | CK | 6.27 ± 0.70$^{a}$ | 5.99 ± 0.29$^{a}$ | 11.40 ± 2.00$^{a}$ | 5.44 ± 0.74$^{a}$ | 5.65 ± 0.13$^{a}$ | 6.68 ± 0.75$^{a}$ |
| | 20 mT | 6.39 ± 0.69$^{a}$ | 5.84 ± 0.26$^{a}$ | 13.07 ± 0.86$^{a}$ | 5.14 ± 0.41$^{a}$ | 5.65 ± 0.21$^{a}$ | 6.74 ± 0.45$^{a}$ |
| | 40 mT | 6.54 ± 0.90$^{a}$ | 6.02 ± 0.39$^{a}$ | 13.08 ± 1.64$^{a}$ | 5.79 ± 1.10$^{a}$ | 5.50 ± 0.05$^{a}$ | 6.26 ± 0.64$^{a}$ |
| | 60 mT | 6.63 ± 0.63$^{a}$ | 5.81 ± 0.31$^{a}$ | 13.08 ± 1.65$^{a}$ | 6.18 ± 0.60$^{a}$ | 6.01 ± 0.69$^{a}$ | 6.37 ± 0.46$^{a}$ |
| | 80 mT | 6.38 ± 0.40$^{a}$ | 5.80 ± 0.24$^{a}$ | 13.08 ± 1.66$^{a}$ | 5.54 ± 1.68$^{a}$ | 5.78 ± 0.48$^{a}$ | 6.22 ± 0.63$^{a}$ |

HS-AP – available phosphorus content at heading stage; RS-AP – available phosphorus content at ripening stage; HS-$NH_4^+$ – $NH_4^+$ content at heading stage; RS-$NH_4^+$ – $NH_4^+$ content at ripening stage; HS-$NO_3^-$ – $NO_3^-$ content at heading stage; RS-$NO_3^-$ – $NO_3^-$ content at ripening stage. Different lowercase letters in the same column at the same soil depth indicate significant differences at $P$ < 0.05

https://doi.org/10.17221/285/2024-PSE

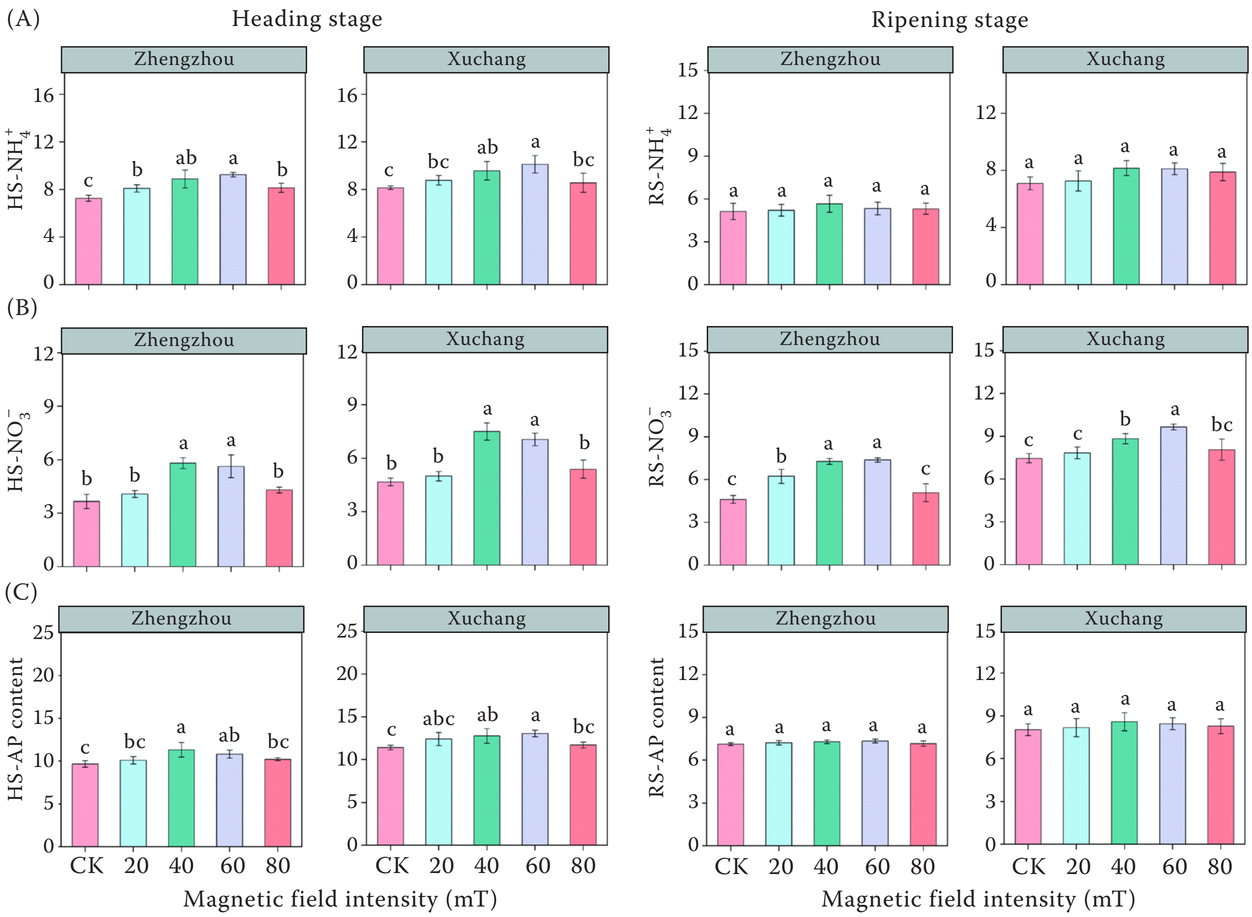


Figure 5. Soil nutrients in wheat rhizosphere at different growth stages. (A) $NH_4^+$-N content at heading (HS) and ripening stage (RS); (B) $NO_3^-$-N content at heading and ripening stage, and (C) AP – available phosphorus content at heading and ripening stage. The significance level was set at $P < 0.05$, with different letters indicating significant differences between different treatments

**Soil nitrogen content ($NH_4^+$-N, $NO_3^-$-N).** At Zhengzhou, at the heading stage, with the increase in magnetic field intensity, the $NO_3^-$-N content first increased and then decreased. At 40 and 60 mT, it significantly increased by 37.7% and 33.7%, respectively, compared with CK, but there was no significant difference from the other treatments. At the ripening stage, it increased by 26.0, 36.7, 37.5, and 9.4% under 20, 40, 60, and 80 mT treatments, respectively, compared to CK. At Xuchang, at the heading stage, there was a significant difference between 40 and 60 mT, with increases of 36.7% and 37.5%, respectively, compared to CK. At the ripening stage, 20, 40, 60, and 80 mT magnetic field treatments increased the soil $NO_3^-$-N content by 26, 36.6, 37.5 and 9.4%, respectively, compared to CK (Figure 5B).

**Soil-available phosphorus.** At the heading stage in Zhengzhou, the AP content significantly increased with increased magnetic field intensity (Figure 5C). When the magnetic field intensity was 20, 40, 60, and 80 mT, the AP content increased by 4.1, 14.6, 10.4, and 5.3%, respectively, compared to CK, and peaked at 40 mT. There was no significant difference at the ripening stage. At Xuchang, at the heading stage, the AP content increased by 24.5% and peaked at 40 mT, while at the ripening stage, the AP content was not significantly different.

**Soil nutrients in bulk soil.** At Zhengzhou, there was no significant difference in AP or $NO_3^-$-N content among different magnetic field treatments in the heading or ripening stages or soil depths (Table 2). At Xuchang, the AP content, $NO_3^-$-N content, and $NH_4^+$-N content at the heading and ripening stages were not significantly different among the magnetic field treatments and soil depths (Table 3).

**Soil bacteria on nutrients.** The analysis of the bacterial community in wheat rhizosphere soil at the heading stage showed that magnetic field treatment

https://doi.org/10.17221/285/2024-PSE

Table 3. Soil nutrient contents in Xuchang of bulk soil

| Soil depth | Treatment | HS-AP | RS-AP | HS-$NH_4^+$ | RS-$NH_4^+$ | HS-$NO_3^-$ | RS-$NO_3^-$ |
|---|---|---|---|---|---|---|---|
| 0–10 cm | CK | 6.18 ± 0.45$^a$ | 5.79 ± 0.22$^a$ | 12.19 ± 1.03$^b$ | 4.91 ± 0.70$^a$ | 6.04 ± 0.74$^a$ | 6.05 ± 0.57$^a$ |
| | 20 mT | 6.53 ± 0.80$^a$ | 5.76 ± 0.11$^a$ | 14.50 ± 0.77$^a$ | 5.26 ± 0.71$^a$ | 5.85 ± 0.63$^a$ | 5.89 ± 0.80$^a$ |
| | 40 mT | 6.88 ± 1.10$^a$ | 5.93 ± 0.23$^a$ | 14.65 ± 1.03$^a$ | 5.40 ± 1.11$^a$ | 6.21 ± 0.75$^a$ | 5.73 ± 6.21$^a$ |
| | 60 mT | 6.72 ± 1.15$^a$ | 5.91 ± 0.27$^a$ | 14.12 ± 0.96$^a$ | 5.99 ± 0.41$^a$ | 5.61 ± 0.72$^a$ | 5.68 ± 0.44$^a$ |
| | 80 mT | 6.51 ± 0.79$^a$ | 5.90 ± 0.22$^a$ | 12.78 ± 0.98$^b$ | 5.23 ± 1.32$^a$ | 5.83 ± 0.80$^a$ | 5.68 ± 0.45$^a$ |
| 10–20 cm | CK | 6.27 ± 0.26$^a$ | 5.88 ± 0.40$^a$ | 13.47 ± 0.88$^c$ | 5.13 ± 0.85$^a$ | 5.32 ± 2.19$^a$ | 5.85 ± 0.61$^a$ |
| | 20 mT | 6.38 ± 0.85$^a$ | 5.93 ± 0.35$^a$ | 14.27 ± 0.61$^{bc}$ | 5.29 ± 0.99$^a$ | 5.46 ± 1.27$^a$ | 5.67 ± 0.47$^a$ |
| | 40 mT | 6.46 ± 0.71$^a$ | 5.91 ± 0.37$^a$ | 15.18 ± 0.50$^{ab}$ | 5.83 ± 0.69$^a$ | 5.49 ± 0.71$^a$ | 5.78 ± 0.58$^a$ |
| | 60 mT | 6.69 ± 1.05$^a$ | 6.20 ± 0.79$^a$ | 15.58 ± 0.97$^a$ | 5.53 ± 0.51$^a$ | 5.58 ± 0.42$^a$ | 5.92 ± 0.71$^a$ |
| | 80 mT | 6.61 ± 0.74$^a$ | 5.97 ± 0.33$^a$ | 14.83 ± 0.93$^{ab}$ | 5.25 ± 0.91$^a$ | 5.60 ± 0.59$^a$ | 5.84 ± 0.61$^a$ |
| 20–30 cm | CK | 6.22 ± 0.50$^a$ | 5.78 ± 0.17$^a$ | 11.90 ± 0.71$^a$ | 5.14 ± 0.41$^a$ | 5.54 ± 0.69$^a$ | 5.80 ± 0.84$^a$ |
| | 20 mT | 6.40 ± 0.65$^a$ | 5.89 ± 0.28$^a$ | 13.41 ± 0.74$^a$ | 5.52 ± 0.82$^a$ | 6.05 ± 0.71$^a$ | 5.62 ± 0.58$^a$ |
| | 40 mT | 6.44 ± 0.73$^a$ | 5.90 ± 0.29$^a$ | 13.08 ± 1.64$^a$ | 5.79 ± 1.10$^a$ | 5.86 ± 0.71$^a$ | 5.83 ± 0.71$^a$ |
| | 60 mT | 6.62 ± 0.64$^a$ | 5.87 ± 0.28$^a$ | 12.37 ± 1.47$^a$ | 5.94 ± 1.00$^a$ | 5.88 ± 0.55$^a$ | 5.94 ± 0.66$^a$ |
| | 80 mT | 6.67 ± 1.17$^a$ | 5.97 ± 0.47$^a$ | 12.09 ± 0.89$^a$ | 5.54 ± 1.68$^a$ | 5.83 ± 0.65$^a$ | 5.94 ± 0.48$^a$ |

HS-AP – available phosphorus content at heading stage; RS-AP – available phosphorus content at ripening stage; HS-$NH_4^+$ – $NH_4^+$ content at heading stage; RS-$NH_4^+$ – $NH_4^+$ content at ripening stage; HS-$NO_3^-$ – $NO_3^-$ content at heading stage; RS-$NO_3^-$ – $NO_3^-$ content at ripening stage. Different lowercase letters in the same column at the same soil depth indicates significant differences at $P < 0.05$

significantly affected community composition. A total of 3 442 microbial species were detected in the two treatments, and 718 species were unique to the magnetic field treatment (Figure 6). The alpha diversity analysis of bacteria showed that the Shannon index and Simpson index of bacteria were significantly affected by magnetic field treatment (Figure 7A). PCA showed that the two treatments were separated on the *X*-axis, indicating they were significantly different (Figure 7B). Correlation analysis of soil nutrient and bacterial alpha diversity showed no significant difference in the soil nutrient or ACE index, but there were significant differences in the soil nutrient and Shannon index at the phylum level. This suggests that the magnetic field treatment significantly affected bacterial community diversity but not community richness (Figure 7C). Correlation analysis of soil nutrient and bacterial beta diversity showed that soil $NH_4^+$-N, $NO_3^-$-N and AP content significantly correlated with bacterial beta diversity (Figure 7D).

RDA analysis of bacteria at the phylum level and soil nutrients showed that, under magnetic field treatment, the AP, $NO_3^-$-N, and $NH_4^+$-N content significantly correlated with bacterial alpha diversity (Figure 8A). The correlation network between soil nutrients and the bacterial community at the genus level in the two treatments showed that 50 bacteria were related to $NO_3^-$-N content, 24 to $NH_4^+$-N content, and 23 to AP content (Figure 8B). We further analysed the abundance of bacteria that affected the AP, $NO_3^-$-N, and $NH_4^+$-N content at the genus level. Magnetic field treatment significantly increased the abundance of *Saccharimonadales* and *Bacteroidetes* and significantly decreased the abun-

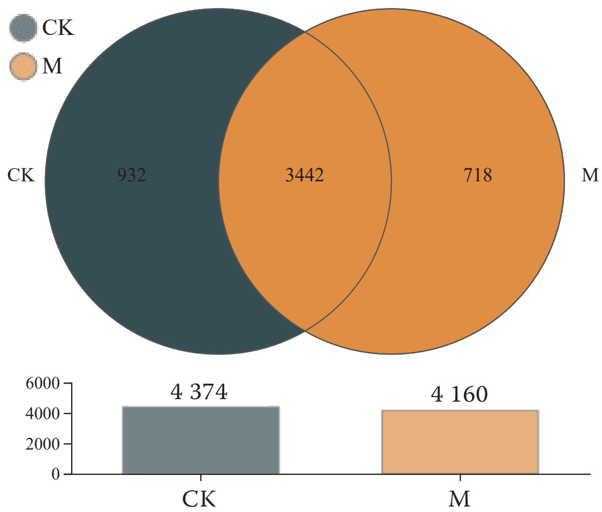


Figure 6. Analysis of species diversity components in different treatments. CK – control; M – 60 mT

https://doi.org/10.17221/285/2024-PSE

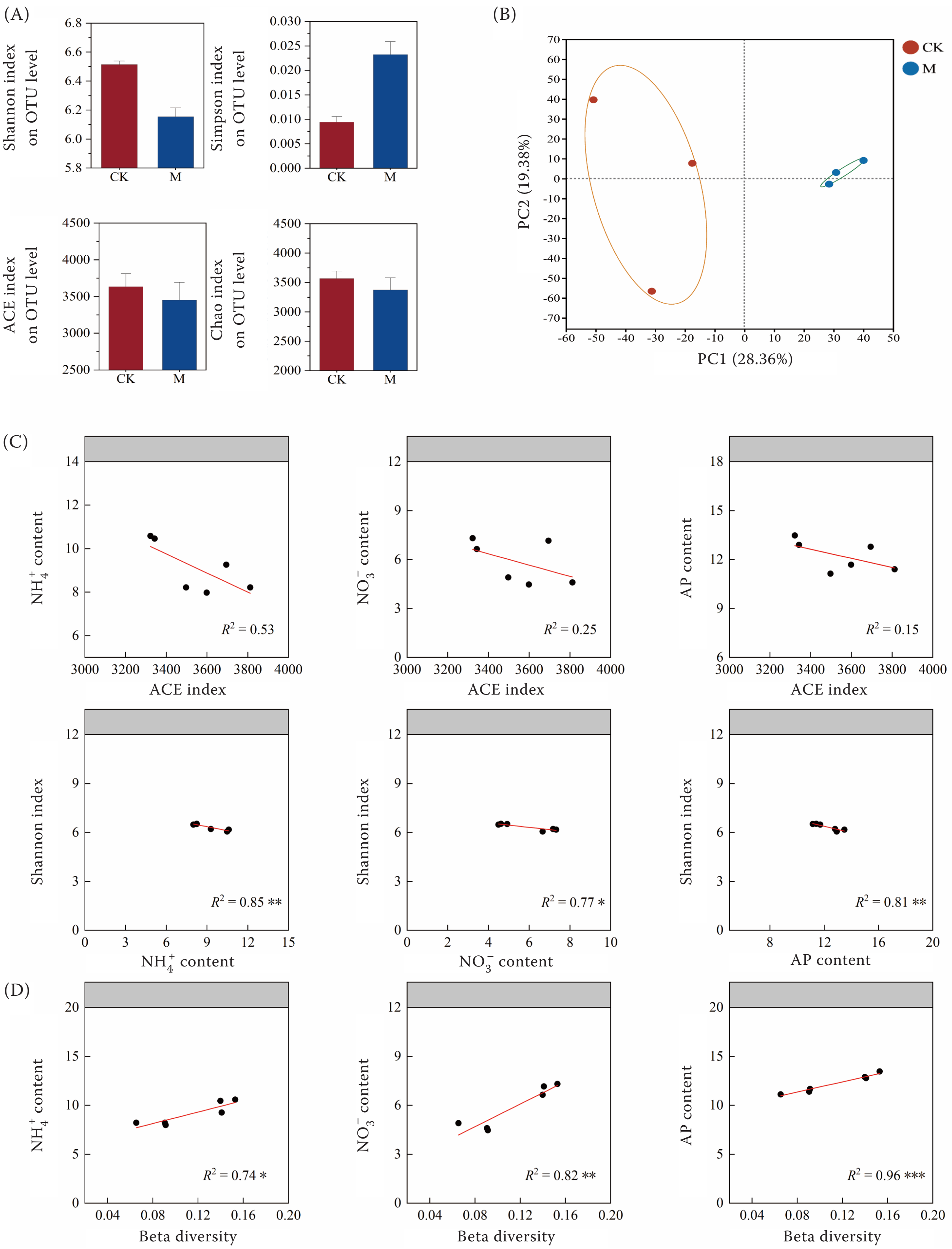


Figure 7. Bacteria alpha diversity in rhizosphere soil at heading stage. (A) Alpha diversity of soil bacteria; (B) PCA analysis; (C) correlation analysis of soil nutrient and bacterial alpha diversity, and (D) correlation analysis of soil nutrient and bacterial beta diversity. *$P$ < 0.05; **$P$ < 0.01; ***$P$ < 0.001; CK – control; M – 60 mT

https://doi.org/10.17221/285/2024-PSE

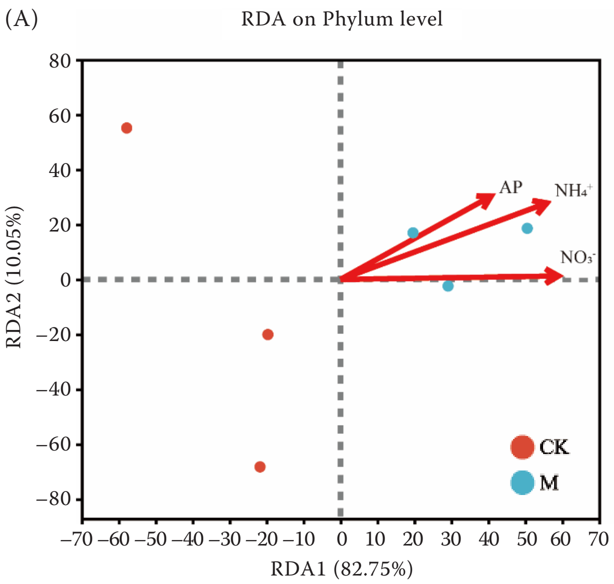


Figure 8. Correlation analysis of main bacteria and soil nutrients. (A) Redundancy analysis (RDA) analysis; (B) correlation network between soil nutrients and bacterial community at genus level; (C) bacterial abundance at genus level affecting (C) $NH_4^+$-N; (D) $NO_3^-$-N and (E) available phosphorus (AP) content at genus level. **P* < 0.05; ***P* < 0.01; CK – control; M – 60 mT

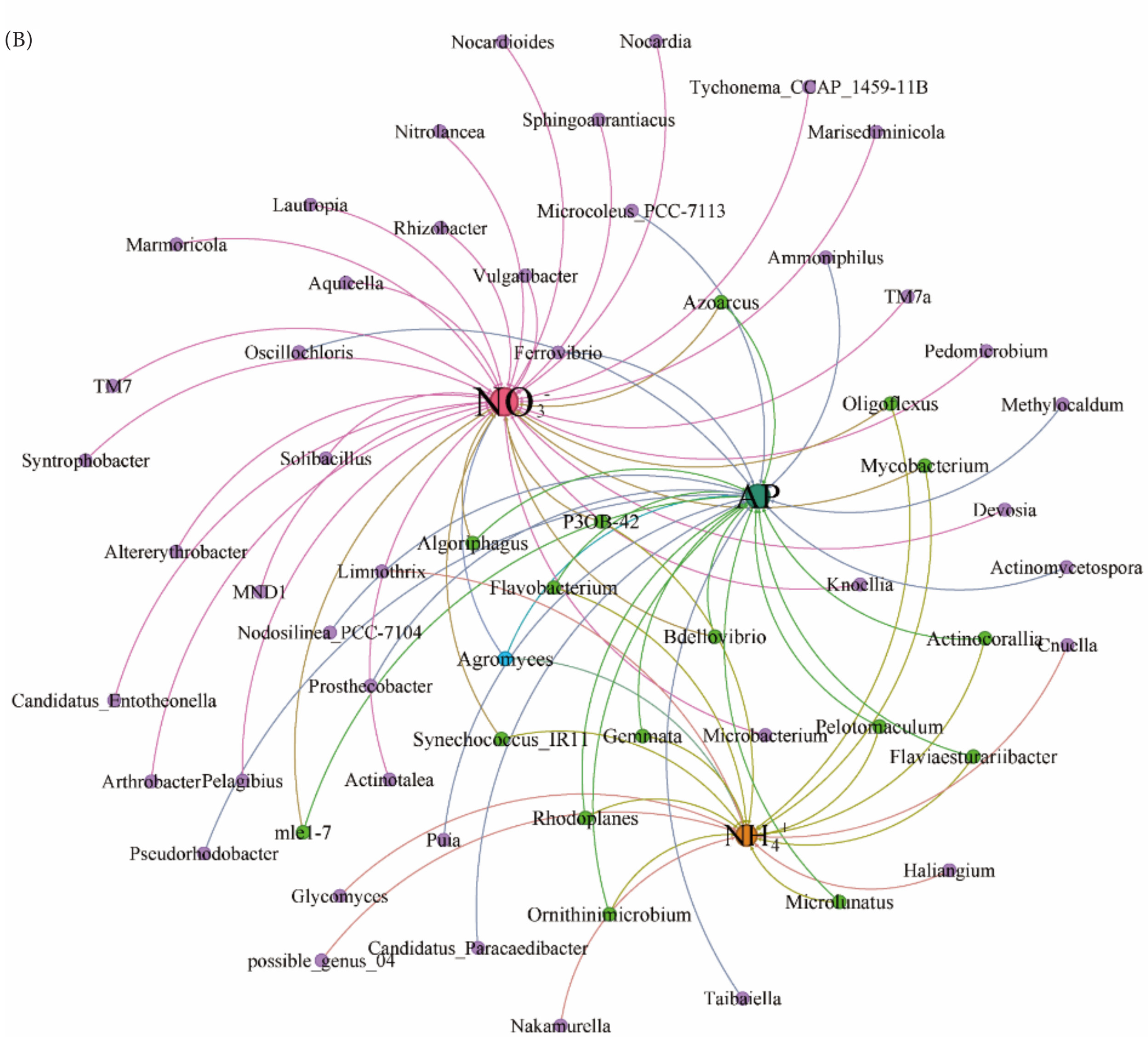

https://doi.org/10.17221/285/2024-PSE

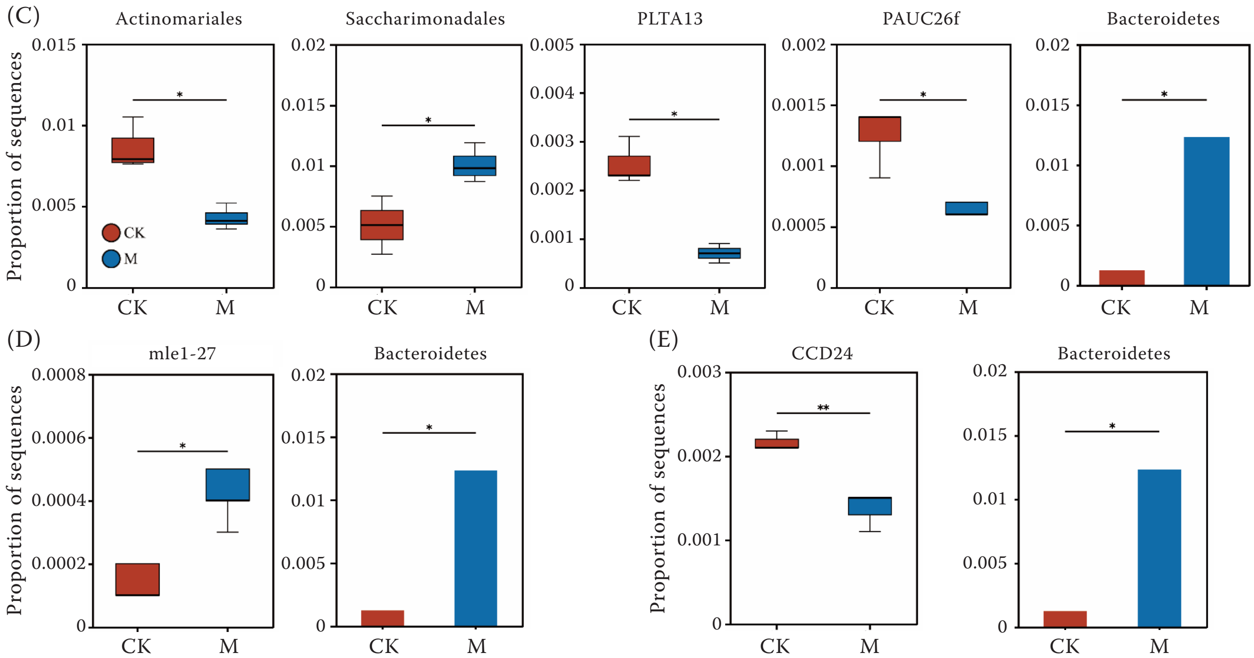


Continued Figure 8. Correlation analysis of main bacteria and soil nutrients. (A) Redundancy analysis (RDA) analysis; (B) correlation network between soil nutrients and bacterial community at genus level; (C) bacterial abundance at genus level affecting (C) $NH_4^+$-N; (D) $NO_3^-$-N and (E) available phosphorus (AP) content at genus level. *$P$ < 0.05; **$P$ < 0.01; CK – control; M – 60 mT

dance of *Actinomarinales*, *PLTA13*, and *PAUC26f* to increase soil $NO_3^-$-N content (Figure 8C), significantly increased the abundance of *mle1-27* and *Bacteroidetes* to increase soil $NH_4^+$-N content (Figure 8D), and significantly decreased the abundance of *CCD24* and increased the abundance of *Bacteroidetes* to increase the AP content (Figure 8E).

**Wheat root morphological parameters.** We analysed the morphological parameters of wheat roots at the heading stage. At Zhengzhou, the root length was

Table 4. Wheat root morphological parameter at heading stage in two sites

| | Treatment | Length (cm) | Surface area ($cm^2$) | Root volume ($cm^3$) | Tips |
|---|---|---|---|---|---|
| Zhengzhou | CK | 4 267.27 ± 88.33$^{c}$ | 503.04 ± 11.67$^{b}$ | 4.47 ± 0.16$^{c}$ | 15 745 ± 914$^{c}$ |
| | 20 mT | 4 400.98 ± 125.55$^{abc}$ | 514.50 ± 16.54$^{ab}$ | 4.68 ± 0.40$^{bc}$ | 16 628 ± 881$^{ab}$ |
| | 40 mT | 4 513.38 ± 108.76$^{ab}$ | 529.31 ± 25.59$^{ab}$ | 5.20 ± 0.46$^{ab}$ | 17 260 ± 818$^{ab}$ |
| | 60 mT | 4 586.65 ± 155.06$^{a}$ | 545.65 ± 28.08$^{a}$ | 5.54 ± 0.29$^{a}$ | 17 555 ± 830$^{a}$ |
| | 80 mT | 4 334.31 ± 131.41$^{bc}$ | 521.22 ± 20.55$^{ab}$ | 4.91 ± 0.25$^{abc}$ | 15 976 ± 565$^{ab}$ |
| ANOVA | *F* | 3.700 | 1.911 | 4.884 | 2.805 |
| | *P* | 0.042 | 0.185 | 0.019 | 0.085 |
| Xuchang | CK | 3 918.80 ± 102.63$^{c}$ | 491.63 ± 13.08$^{c}$ | 3.96 ± 0.38$^{b}$ | 12 987 ± 617$^{a}$ |
| | 20 mT | 4 001.17 ± 165.37$^{bc}$ | 509.29 ± 19.45$^{ab}$ | 4.73 ± 0.41$^{a}$ | 13 349 ± 686$^{a}$ |
| | 40 mT | 4 218.62 ± 118.96$^{ab}$ | 522.75 ± 22.59$^{ab}$ | 4.90 ± 0.32$^{a}$ | 13 949 ± 808$^{a}$ |
| | 60 mT | 4 287.36 ± 179.38$^{a}$ | 531.25 ± 16.77$^{a}$ | 4.97 ± 0.37$^{a}$ | 14 247 ± 422$^{a}$ |
| | 80 mT | 4 176.61 ± 112.37$^{abc}$ | 513.98 ± 20.45$^{ab}$ | 4.81 ± 0.36$^{a}$ | 13 322 ± 743$^{a}$ |
| ANOVA | *F* | 3.301 | 1.692 | 3.706 | ns |
| | *P* | 0.057 | 0.228 | 0.042 | 0.213 |

Different lowercase letters in the same column at the same soil depth indicate significant differences. Significance levels are as follows: *$P$ < 0.05; **$P$ < 0.01; ns – not significant

https://doi.org/10.17221/285/2024-PSE

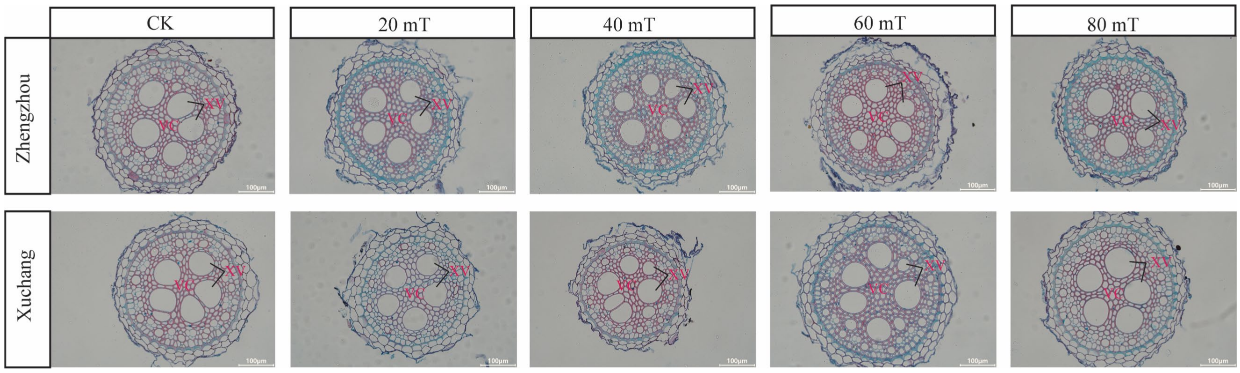


Figure 9. Ultrastructure of root section in two sites. XV – xylem vessel; VC – vascular cylinder; CK – control

significantly different under 40 and 60 mT magnetic field treatments compared to CK; it increased by 7.11% and 8.60%, respectively. The root volume also showed a significant difference; with magnetic field treatment at 40 and 60 mT, it increased by 14.07% and 19.31%, respectively. At Xuchang, magnetic field treatment also significantly promoted root length at 40 and 60 mT; it increased by 5.45% and 6.96%, respectively. All four magnetic field treatments increased the root volume; it increased 16.25, 19.29, 20.40, and 17.66% at 20, 40, 60, and 80 mT, respectively, compared to CK (Table 4).

At the heading stage, wheat roots were collected to observe the ultramicroscopic and microstructure of root cross-sections, and the cortex, vascular cylinder, vessel, and phloem were observed. When the magnetic field intensity reached 60 mT, the area of the vascular cylinder became larger and more xylem vessels were differentiated compared to CK. Under magnetic field treatment, the root system had a good

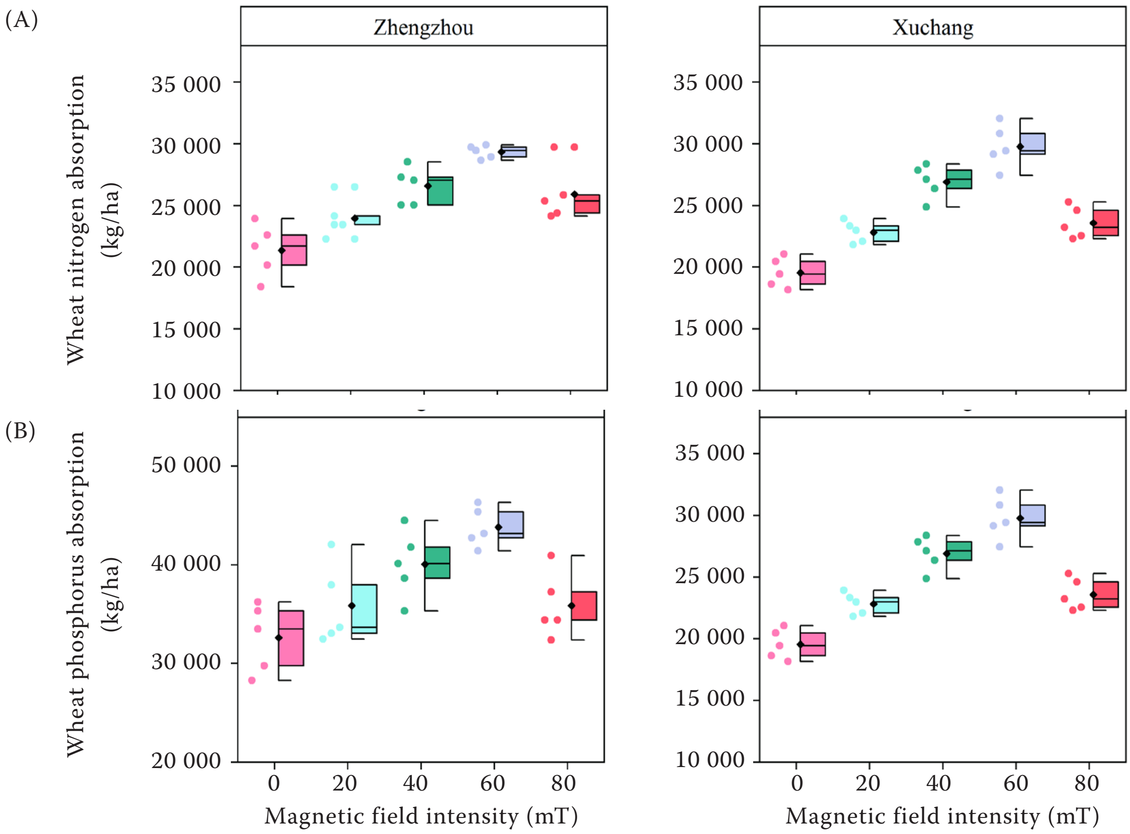


Figure 10. Wheat plants nitrogen and phosphorus absorption content at ripening stage in two sites. (A) Wheat nitrogen absorption content, and (B) wheat phosphorus absorption content

https://doi.org/10.17221/285/2024-PSE

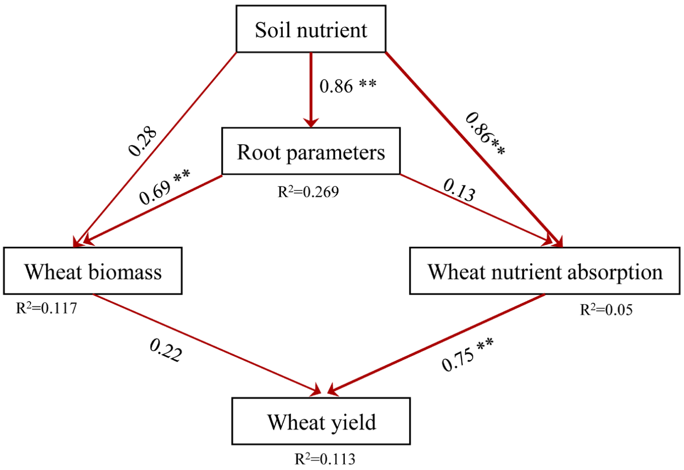


$\chi^2$ = 73.509; CFI – 0.911; *P* = 0.052; RMSEA = 0.243

Figure 11. Structural equation modeling (SEM) analysis. It shows the relationships between soil nutrients ($NO_3^-$-N, $NH_4^+$-N and available phosphorus (AP) content), root parameter: root length, root surface, root volume and tips), wheat nutrient absorption, wheat biomass and wheat yield. The width of the arrows is proportional to the strength of path coefficients, and the numbers adjacent to arrows are standardised path coefficients. Significance levels are as follows: $^*P < 0.05$; $^{**}P < 0.01$; $R^2$ – proportion of variance explained and appears near every response variable in the model. Model fitness details ($\chi^2$, degrees of freedom, *P*-value, and RMSEA – root mean square error of approximation; CFI – comparative fit index) are close to the figure

shape, which manifested as more regular cell shapes in the cross-section and a clearer epidermis, cortex, and vascular bundle. The cortical thickness was large, with a neat and dense cell arrangement. There were more complete structures in the vascular bundle at the root tip, and the neatly arranged ducts and pith were clearly visible (Figure 9).

**Wheat nitrogen and phosphorus content**. The wheat nitrogen and phosphorus absorption content was significantly increased under magnetic field treatment. At Zhengzhou, the wheat nitrogen absorption content was significantly increased by 14.35, 27.36, 34.34, and 17.12% compared to CK when the magnetic field intensity was at 20, 40, 60, and 80 mT, respectively. Wheat phosphorus absorption content also had a significant difference; it increased by 9.56, 26.14, 31.98, and 11.40% under the 20, 40, 60, and 80 mT treatments, respectively. At Xuchang, the wheat nitrogen absorption content increased by 10.84, 19.63, 27.14, and 17.48% under the 20, 40, 60, and 80 mT treatments, respectively, compared to CK. The wheat phosphorus absorption content increased by 8.99, 18.57, 25.50 and 9.05% under 20, 40, 60, and 80 mT magnetic field intensities, respectively, compared with CK (Figure 10).

**SEM analysis.** Our SEM analysis showed that soil nutrients (AP, $NO_3^-$-N, and $NH_4^+$-N content) significantly affected wheat nutrient absorption (wheat nitrogen and phosphorus absorption), and wheat nutrient absorption significantly affected wheat yield (Figure 11). Soil nutrients also significantly affected root parameters (root length, root surface area, root volume, root tips), and the root parameters had positive effects on the contribution of wheat biomass. Taken together, the magnetic field significantly affected soil nutrients, in turn affecting wheat nutrient absorption (0.86**) and wheat yield (0.75**). Additionally, the soil nutrient effect on root parameters (0.86**) affected wheat biomass (0.69**), which then affected wheat yield (0.22).

## DISCUSSION

**Magnetic field treatment of wheat biomass, wheat yield, and yield components.** Our two-site study found that magnetic field treatment significantly increased wheat biomass and yield, confirming hypothesis 1 and suggesting that the magnetic field treatment can be used to increase wheat yield as a new method, and there are some previous reports on the effect of magnetic field on crop growth, some study showed that magnetic treatment before sowing applied to dry wheat seeds enhanced the growth of the wheat plant and improved their fruit yield and yield parameters due to increasing in plant nutrients (Hussain et al. 2020). But how the magnetic field can actually be applied to agricultural production is worth considering, because increasing the intensity of the magnetic field in the field for a long time requires a huge energy input, which seems unrealistic. However, short-term high-intensity magnetic field treatment is feasible and has been successfully applied in seed treatment, food production, environmental modification and so on (Bhardwaj et al. 2012, Mshenskaya et al. 2023). The current question is what is the mechanism by which magnetic fields promote wheat growth? This is a complex problem, which may be related to the influence of magnetic

https://doi.org/10.17221/285/2024-PSE

field on wheat growth and development, and may also be related to the influence of magnetic field on wheat growth environment. Our study focuses on the effect of magnetic fields on soil nutrient environments. We found that the increase in yield was closely related to the increase in soil main nutrient content, such as nitrogen and phosphorus, in rhizosphere soils and SEM analysis also showed that soil nutrients significantly affected wheat nitrogen and phosphorus uptake and that wheat nitrogen and phosphorus uptake significantly affected wheat yield.

**Effect of a magnetic field on soil nitrogen and phosphorus content.** In the present study, we measured soil available nutrient content in rhizosphere soil and bulk soil. There was no significant difference in bulk soil among the different soil depths. This suggests that the magnetic field mainly affects the nutrient content in wheat rhizosphere soil. This may be because the nutrient conversion process in the rhizosphere was more active under magnetic field treatment (Katrin et al. 2010). In our study, soil $NH_4^+$-N, $NO_3^-$-N, and AP contents at the heading stage were significantly different under different magnetic field treatments. Previous research confirms that the rhizosphere process can significantly affect soil nutrient transformation (Phillips et al. 2011, Zhu et al. 2014, Yin et al. 2018), and that bacterial activities may promote soil nutrient transformation (Jilling et al. 2018). Bacteria in rhizosphere soils are an important part of soil microbial communities and can promote energy exchange between roots and soil (Zhang et al. 2023). In our study, magnetic field treatment significantly affected the rhizosphere bacterial community diversity but not community richness. Furthermore, the analysis of bacterial communities showed that the change in soil nutrients was caused by the change in soil bacterial community diversity but not community richness after magnetic treatment. The results showed that magnetic fields could alter the diversity of rhizosphere microorganisms in wheat, affecting nutrient availability. This effect has also been reported in some studies. For example, the previous study showed that improving microbial diversity effectively enhanced microbial nutrient conversion (Zhouchang et al. 2023). We further determined the relationship between microorganisms and $NO_3^-$-N, $NH_4^+$-N and AP, it indicated that magnetic field treatment significantly increased the abundance of *Saccharimonadales* and *Bacteroidetes* and significantly decreased the abundance of *Actinomarinales*, *PLTA13*, and *PAUC26f* to increase the soil $NO_3^-$-N content, significantly increased the abundance of *mle1-27* and *Bacteroidetes* to increase the soil $NH_4^+$-N content, and significantly decreased the abundance of *CCD24* and increased the abundance of *Bacteroidetes* to increase the AP content. In summary, we have preliminarily analysed the microbial effects of magnetic field on soil N and P, and it may be necessary to further study the microbial effects of magnetic field on promoting soil available nutrients in combination with microbial functions in the future.

**Effect of a magnetic field on root characteristics and wheat nitrogen and phosphorus absorption.** In this study, the increase in soil rhizosphere nutrient content was accompanied by the promotion of root growth. We speculate that the magnetic field may enhance the activation capacity of rhizosphere soils and promote an increase in nitrogen and phosphorus content in the rhizosphere. Previous studies have shown that the transformation process of nutrients is faster in plant roots (Fan et al. 2018). An adequate nutrient supply promotes root growth, as found in our study. The parameters of root scanning and the ultrastructure of root morphology showed that magnetic field treatment promoted the growth of wheat roots at the heading stage. The increase in total root length and root surface area under magnetic field treatment may be the result of increased stimulative effects on plant photosynthesis and growth (Zhang et al. 2015, Li et al. 2020). Previous studies have shown that magnetic field treatment can boost crop photosynthesis (Shine and Guruprasad 2012, De Souza-Torres et al. 2020). Some photosynthates are translocated belowground for root growth and maintenance (Pii et al. 2015, Zhu et al. 2016). The nitrogen and phosphorus content in wheat plants at the heading stage showed that both nitrogen and phosphorus uptake increased under magnetic field treatment. We speculate that a magnetic field affects the absorption of soil nutrients by roots and increases the absorption of nitrogen and phosphorus by plants, thus promoting wheat growth and increasing yield. This is consistent with some studies that have shown that an increase in wheat biomass is related to an increase in nutrient use efficiency at the heading stage. Large roots facilitate nitrogen uptake in wheat, and a higher root length density may also increase nutrient uptake (Pang et al. 2015). Nutrients transported to wheat plants and their products, including nitrate $NH_4^+$-N and $NO_3^-$-N, are absorbed by plants, affecting the nutrient input and production of plants (Wardle et al. 2004, Bardgett et al. 2005).

https://doi.org/10.17221/285/2024-PSE

These results demonstrated that magnetic fields had positive effects on wheat fields, suggesting that magnetic fields could change soil bacterial community diversity and bacterial abundance to increase soil nutrients and wheat yield. Our findings preliminarily verified the effect of magnetic field on wheat growth, confirmed the effect of magnetic field on rhizosphere available nutrients, and clarified the relationship between nutrient enhancement and microorganisms, would have important implications for efficient and green agricultural production.

## REFERENCES


Alpsoy H.C., Unal H. (2019): Effect of stationary magnetis field on seed germination and crop yield in spinach (*Spinacia oleracea* L.). Comptes rendus de l'Academie bulgare des Sciences, 72: 687–696.

Arata A.F., Lázaro L., Tranquilli G.E., Arrigoni A.C., Martínez M., Rondanini D.P. (2023): How does post-flowering source/sink manipulation affect grain weight and commercial quality in Argentinean bread wheat genotypes with different baking aptitude? Field Crops Research, 301: 109030.

Bardgett R.D., Bowman W.D., Kaufmann R., Schmidt S.K. (2005): A temporal approach to linking aboveground and belowground ecology. Trends in Ecology and Evolution, 20: 634–641.

Barillot C.D.C., Sarde C.O., Bert V., Tarnaud E., Cochet N. (2013): A standardized method for the sampling of rhizosphere and rhizoplan soil bacteria associated to a herbaceous root system. Annals of Microbiology, 63: 471–476.

Bhardwaj J., Anand A., Nagarajan S. (2012): Biochemical and biophysical changes associated with magnetopriming in germinating cucumber seeds. Plant Physiology and Biochemistry, 57: 67–73.

Chen X., Fang K., Chen C. (2012): Seasonal variation and impact factors of available phosphorus in typical paddy soils of Taihu Lake region, China. Water and Environment Journal, 26: 392–398.

Chen Y., Chen D., Liu Q. (2017): Exposure to a magnetic field or laser radiation ameliorates effects of Pb and Cd on physiology and growth of young wheat seedlings. Journal of Photochemistry and Photobiology B-Biology, 169: 171–177.

Covacevich F., Echeverría H.E., Aguirrezabal L.A.N. (2007): Soil available phosphorus status determines indigenous mycorrhizal colonization of field and glasshouse-grown spring wheat from Argentina. Applied Soil Ecology, 35: 1–9.

Dai J., He G., Wang S., Cao H., Hui X., Ma Q., Liu J., Siddique K.H.M., Wang Z., Sadras V.O. (2022): Matching NPK fertilization to summer rainfall for improved wheat production and reduced environmental cost. Field Crops Research, 286: 108613.

De Souza-Torres A., Sueiro-Pelegrin L., Zambrano-Reyes M., Macias-Socarras I., Gonzalez-Posada M., Garcia-Fernandez D. (2020): Extremely low frequency non-uniform magnetic fields induce changes in water relations, photosynthesis and tomato plant growth. International Journal of Radiation Biology, 96: 951–957.

De V.F.T., Griffiths R.I., Mark B., Hayley C., Mariangela G., Soon G.H., Sara H., Aurore K., Keith A.M., Marina K. (2018): Soil bacterial networks are less stable under drought than fungal networks. Nature Communications, 9: 3033.

Fan K., Weisenhorn P., Gilbert J.A., Chu H. (2018): Wheat rhizosphere harbors a less complex and more stable microbial co-occurrence pattern than bulk soil. Soil Biology and Biochemistry, 125: 251–260.

Fu Q., Yan J., Li H., Li T., Hou R., Liu D., Ji Y. (2019): Effects of biochar amendment on nitrogen mineralization in black soil with different moisture contents under freeze-thaw cycles. Geoderma, 353: 459–467.

Ghanati F., Payez A. (2015): Iron biofortification and activation of antioxidant system of wheat by static magnetic field. Iranian Journal of Science and Technology Transaction A – Science, 39: 355–360.

Hussain M.S., Dastgeer G., Afzal A.M., Hussain S., Kanwar R.R. (2020): Eco-friendly magnetic field treatment to enhance wheat yield and seed germination growth. Environmental Nanotechnology Monitoring and Management, 14: 100299.

Jilling A., Keiluweit M., Contosta A.R., Frey S., Schimel J., Schnecker J., Smith R.G., Tiemann L., Grandy A.S. (2018): Minerals in the rhizosphere: overlooked mediators of soil nitrogen availability to plants and microbes. Biogeochemistry, 139: 103–122.

Jyolsna T., Vashisht B.B., Yadav M., Kaur R., Jalota S.K. (2024): Field and simulation studies on yield, water and nitrogen dynamics and use efficiency in rice-wheat crops in sequence. Field Crops Research, 311: 109366.

Katrin G., Evelyn H., Erich I., Joseph S., Wolfgang W., Sophie Z.B., Angela S. (2010): Dynamics of ammonia-oxidizing communities in barley-planted bulk soil and rhizosphere following nitrate and ammonium fertilizer amendment. FEMS Microbiological Ecology, 74: 575–591.

Li Y.Y., Xu Y., Li Y.L., Wu T., Zhou G., Liu S., Meng Y., Wang J., Ling L., Liu J. (2020): Warming effects on morphological and physiological performances of four subtropical montane tree species. Annals of Forest Science, 77: 2.

Liu L., Hu C., Olesen J.E., Ju Z., Yang P., Zhang Y. (2013): Warming and nitrogen fertilization effects on winter wheat yields in northern China varied between four years. Field Crops Research, 151: 56–64.

Kuypers M.M.M., Marchant H.K., Kartal B. (2018): The microbial nitrogen-cycling network. Nature Reviews Microbiology, 16: 263–276.

Merloti L.F., Mendes L.W., Pedrinho A., de Souza L.F., Ferrari B.M., Tsai S.M. (2019): Forest-to-agriculture conversion in Amazon drives soil microbial communities and N-cycle. Soil Biology and Biochemistry, 137: 107567.

Mshenskaya N.S., Grinberg M.A., Kalyasova E.A., Vodeneev V.A., Ilin N.V., Slyunyaev N.N., Mareev E.A., Sinitsyna Y.V. (2023): The effect of an extremely low-frequency electromagnetic field on the drought sensitivity of wheat plants. Plants-Basel, 12: 826.

Olsen S.R. (1954): Estimation of Available Phosphorus in Soils by Extraction with Sodium Bicarbonate. Washington, US Department of Agriculture, Circ., 939.

Pang J., Stephen P.M.A., Rebetzke G.J., Palta J.A. (2015): The influence of shoot and root size on nitrogen uptake in wheat is affected by nitrate affinity in the roots during early growth. Functional Plant Biology, 42: 1179–1189.

Phillips R.P., Finzi A.C., Bernhardt E.S. (2011): Enhanced root exudation induces microbial feedbacks to N cycling in a pine forest under long-term $CO_2$ fumigation. Ecology Letters, 14: 187–194.

Pietruszewski S., Kania K. (2010): Effect of magnetic field on germination and yield of wheat. International Agrophysics, 24: 297–302.

Pii Y., Mimmo T., Tomasi N., Terzano R., Cesco S., Crecchio C. (2015): Microbial interactions in the rhizosphere: beneficial influences of plant growth-promoting rhizobacteria on nutrient acquisition process. A review. Biology and Fertility of Soils, 51: 403–415.

Shine M.B., Guruprasad K.N. (2012): Impact of pre-sowing magnetic field exposure of seeds to stationary magnetic field on growth, reactive oxygen species and photosynthesis of maize under field conditions. Acta Physiologiae Plantarum, 34: 255–265.

Song Y., Li X., Yao S., Yang X., Jiang X. (2020): Correlations between soil metabolomics and bacterial community structures in the pepper rhizosphere under plastic greenhouse cultivation. Science of The Total Environment, 728: 138439.

Sukhov V., Sukhova E., Sinitsyna Y., Gromova E., Mshenskaya N., Ryabkova A., Ilin N., Vodeneev V., Mareev E., Price C. (2021): Influence of magnetic field with Schumann resonance frequencies on photosynthetic light reactions in wheat and pea. Cells, 10: 149.

Trivedi P., Leach J.E., Tringe S.G., Sa T., Singh B.K. (2021): Author correction: plant-microbiome interactions: from community assembly to plant health. Springer Science and Business Media, LLC(1): 72.

Wardle D.A., Bardgett R.D., Klironomos J.N., Setälä H., van der Putten W.H., Wall D.H. (2004): Ecological linkages between aboveground and belowground biota. Science, 304: 1629–1633.

Yan S., Wu Y., Fan J., Zhang F., Zheng J., Qiang S., Wu L. (2020): Dynamic change and accumulation of grain macronutrient (N, P and K) concentrations in winter wheat under different drip fertigation regimes. Field Crops Research, 250: 107767.

Yin L., Dijkstra F.A., Wang P., Zhu B., Cheng W. (2018): Rhizosphere priming effects on soil carbon and nitrogen dynamics among tree species with and without intraspecific competition. New Phytologist, 218: 1036–1048.

Zhang K., Shi Y., Cui X., Yue P., Li K., Liu X., Tripathi B.M., Chu H., Lozupone C. (2019): Salinity is a key determinant for soil microbial communities in a desert ecosystem. mSystems, 4: 1.

Zhang N., Wan S., Guo J., Han G., Gutknecht J., Schmid B., Yu L., Liu W., Bi J., Wang Z., Ma K. (2015): Precipitation modifies the effects of warming and nitrogen addition on soil microbial communities in northern Chinese grasslands. Soil Biology and Biochemistry, 89: 12–23.

Zhang W., Zhou Y., Li C., Zhu K., Xu Y., Wang W., Liu L., Zhang H., Gu J., Wang Z., Zhang J., Yang J. (2022): Post-anthesis moderate soil-drying facilitates source-to-sink remobilization of nitrogen *via* redistributing cytokinins in rice. Field Crops Research, 288: 108692 .

Zhang Y., Xu S., Liu G., Lian T., Li Z., Liang T., Zhang D., Cui Z., Zhan L., Sun L., Nie J., Dai J., Li W., Li C., Dong H. (2023): Ridge intertillage alters rhizosphere bacterial communities and plant physiology to reduce yield loss of waterlogged cotton. Field Crops Research, 293: 108849.

Zhang Y.H., Song M., Zhu Y., Li H., Zhang Y.L., Wang G., Chen X., Zhang W., Wang H., Wang Y., Shao R., Guo J., Yang Q. (2024): Impact of microplastic particle size on physiological and biochemical properties and rhizosphere metabolism of *Zea mays* L.: comparison in different soil types. Science of The Total Environment, 908: 168219.

Zhouchang Y., Wei Z., Liyun Z., Shihai M., Lin S., Yushu L., Ling C. (2023): Efficient vegetation restoration in Mu Us desert reduces microbial diversity due to the transformation of nutrient requirements. Ecological Indicators, 154: 110758.

Zhu B., Gutknecht J., Herman D.J., Keck D.C., Firestone M.K., Cheng W. (2014): Rhizosphere priming effects on soil carbon and nitrogen mineralization. Soil Biology and Biochemistry, 76: 183–192.

Zhu Z., Zeng G., Ge T., Hu Y., Wu J. (2016): Fate of rice shoot and root residues, rhizodeposits, and microbe-assimilated carbon in paddy soil: I. Decomposition and priming effect. Biogeosciences Discussions, 13: 4481–4489.

Received: May 28, 2024
Accepted: August 20, 2024
Published online: September 20, 2024